Perovskite $Sr_{0.9}Fe_{0.9}Zr_{0.1}O_{3-\delta}$: Redox-stable Structure, Oxygen Vacancy, Electrical Properties and Steam Electrolysis Performance

LI Zhe (李 哲);YE Ling-Ting (叶灵婷);XIE Ku(谢 奎)

CAS Key Laboratory of Design and Assembly of Functional Nanostructures, and Fujian Provincial Key Laboratory of Nanomaterials, Fujian Institute of Research on the Structure of Matter, Chinese Academy of Sciences, Fuzhou 350002, *China*

ABSTRACT Many researchers have studied on perovskite oxide for its unique structure. Perovskite oxides, $ABO_{3-\delta}$, with different A and B metals have shown wide applications in many fields, in particular solid oxide electrolysers. $SrFeO_{3-\delta}$, typical perovskite oxides, in which iron is the mixed-valence cation with the capacity to change the chemical valence, have a wide range of oxygen nonstoichiometry. In this study, $Sr_{0.9}Fe_{0.9}Zr_{0.1}O_{3-\delta}$ (SFZO) is synthesized and then treated in 5%H_2/Ar and air at high temperature, exhibiting excellent redox stability. Redox-stable structure, oxygen vacancy and electrical properties of SFZO are investigated. Steam electrolysis is then performed with SFZO cathode under 5%H_2O/5%H_2/Ar and 5%H_2O/Ar atmospheres, respectively. The present results indicate that the SFZO is a novel promising cathode material for solid oxide steam electrolyser.

Keywords: phase structure; solid oxide electrolyser; $Sr_{0.9}Fe_{0.9}Zr_{0.1}O_{3-\delta}$; cathode; steam electrolysis;
DOI: 10.14102/j.cnki.0254-5861.2011-1716

1 INTRODUCTION

The perovskite oxides, $ABO_{3-\delta}$, have attracted numerous attention for many years due to the unique structure. Perovskite-type oxides have a large flexibility of the structure, in which the valence state of mixed-valence transition metal (TM) cations could change to some extent, as well as the number of oxygen vacancies[1-3]. Meanwhile, $ABO_{3-\delta}$ oxides have exhibited fascinating properties, and have been studied on many fields such as oxygen permeable membranes[4], photocatalysis[5], magnetic materials[6], solid oxide fuel cells (SOFCs)[7] and solid oxide electrolysis cells (SOECs)[8].

$SrFeO_{3-\delta}$, typical perovskite oxides, contain mixed-valence iron cations presented as Fe^{4+} in B-site that could transform to lower valence state at low oxygen partial pressure accompanied by the formation of oxygen vacancies[9]. It is no doubt that the phase structure of strontium ferrates can transform, at relatively stronger reducing atmosphere, from cubic to orthorhombic brown millerite phase, in which oxygen vacancies aggregate and ultimately represent ordering[10]. Oxygen vacancies usually exist in perovskites as point defects, and have nonnegligible influence on its structure and electronic properties. The appropriate amount of oxygen vacancies is in favour of the oxygen-ion transmission, resulting in good electronic properties; whereas, a sufficiently high concentration of oxygen vacancies is not favourable as it can aggregate, arrange orderly and even give rise to phase transformation. As a result, the oxide ion conduction and electrical conductivity are drastically reduced[11].

In this work, the Zr-doping perovskite $Sr_{0.9}Fe_{0.9}Zr_{0.1}O_{3-\delta}$ (SFZO) is synthesized by solid state reaction method to suppress the phase transition. The structure, oxygen vacancies, electrical properties and electrochemical properties of SFZO are systematically studied. Steam electrolysis is then performed with SFZO cathode.

2 EXPERIMENTAL

2. 1 Materials and apparatus

Perovskite $Sr_{0.9}Fe_{0.9}Zr_{0.1}O_{3-\delta}$ (SFZO) powder was prepared by a traditional solid-state reaction method. Stoichiometric $SrCO_3$, Fe_2O_3 and ZrO_2 (all chemicals used in this current investigation were 99% AR from Sinopharm Chemical Reagent Co., Ltd) were completely mixed by grounding in a zirconia ball mill for 10 min at a speed of 1000 rounds per min, and then pressed into pellets followed by calcination in air at 1300 ºC for 20 h. The SFZO samples were reduced in 5%H_2/Ar at 800 ºC for 3 h.

The phase analysis of the as-synthesized SFZO powder was performed by X-ray diffraction (XRD) at room temperature using D/MAX2500V, Rigaku Corporation, Japan (Cu$K\alpha$, 2θ = 20~80 °) at a scan rate of 3 °$\cdot$min^{-1}. The surface microstructure of the electrolyser was observed by Scanning Electron Microscopy (SEM, JSM-6490LV, JEOL Ltd, Japan). Transmission Electron Microscopy analysis (TEM) was used to investigate the oxidized SFZO powder with a JEOL 2100F field emission transmission electron microscope operating at 200 kV. X-ray photoelectron spectroscopy (XPS, Al$K\alpha$, ESCALAB25, Thermo, America) was employed to analyze the chemical state of the elements on SFZO surface before and after high temperature treatment in 5%

H_2/Ar at 800 ºC for 3 h. TGA testing of the reduced SFZO powder was conducted using a thermal analyzer in air with the temperature changing from 320 to 1000 ℃ in a speed of 5 ºC min^{-1} (STA449F3, Naichi Corporation, Germany). The conductivities of samples were measured with a direct current four-probe method by an electrochemical workstation (Keithley 2000, Digital Multimeter, Keithley Instruments Inc., USA) in the air atmosphere and reducing (5%H_2/Ar) atmosphere with temperature ranging from 650 to 800 ºC, respectively. The dependence of conductivity on the oxygen partial pressure was measured at 800 ºC by an online multimeter (Keithley 2000, Digital Multimeter, Keithley Instruments Inc., USA) and the oxygen partial pressure ranging from 10^{-17} to 10^{0} atm was recorded by online oxygen sensor (OXYGEN-MODEL 3000-SX).

2. 2 Symmetrical cells preparation

The 2-mm-thick 8YSZ electrolyte support was prepared by dry-pressing the 8YSZ powders into a disk with a diameter of 20 mm followed by sintering in air at 1550 ºC for 20 h. Two surfaces of the YSZ electrolyte support were mechanically polished and ultrasonically cleaned in ethanol and acetone. The $Ce_{0.8}Sm_{0.2}O_{2-\delta}$ (SDC) powders were prepared by the combustion method in which the Sm_2O_3 and $Ce(NO_3)_3$ $6H_2O$ powders were mixed evenly and sintered at 800 ºC (3 ºC min^{-1}) for 3 h in air. The cathode slurry of SFZO-SDC was formed by mixing the prepared SFZO-SDC powder (at a ratio 65:35 wt%), alpha-terpineol, and appropriate amounts of cellulose additive. Then the cathode slurry was printed onto the two surfaces of the prepared cleaned YSZ discs with an area of approximately 0.5 cm^2, followed by sintering in air at 1100 ºC for 3 h to assemble symmetrical cells. Ag paste (SS-8060, Xinluyi, Shanghai, China) was used as a current collector covering anode and cathode surfaces, and Ag wire (0.2 mm in diameter) was used for connecting the electrodes to the electrochemical equipment, followed by firing in air at 550 ºC for 30 min. The symmetrical cells (SFZO-SDC/YSZ/SFZO-SDC) were measured by the electrochemical workstation (IM6, Zahner, Germany) at open circuit voltage (OCV) at 800 ºC under different hydrogen partial pressure and different oxygen partial pressure, respectively. The applied frequency was in the range of 100 mHz~4 MHz, with a voltage amplitude of 10 mV. The flow rate of gas was 50 ml min^{-1}, controlled by a mass flow meter (D08-5F, Sevenstar, Beijing, China).

2. 3 Electrolysis cells preparation

The powders of $(La_{0.8}Sr_{0.2})_{0.95}MnO_{3-\delta}$ (LSM) were synthesized using solid state reaction by mixing the proper amounts of La_2O_3, $SrCO_3$ and MnO_2 and the treatment temperature was 1100 ºC (3 ºC min^{-1}) for 10 h in air. The LSM slurry was formed by mixing the prepared LSM-SDC powder (at a ratio 65:35 wt%),

alpha-terpineol, and appropriate amounts of cellulose additive. Then the SFZO-SDC slurry was printed onto the cathode surfaces and the LSM slurry onto the anode surfaces of YSZ discs with an area of approximate 0.2 cm^2, respectively, followed by sintering in air for 3 h at 1100 ºC to assemble the single solid oxide cells (SFZO-SDC/YSZ/LSM-SDC). The single solid-oxide electrolysers were sealed by ceramic paste (JD-767A, Jiudian, Dongguan, China) to a home-made testing apparatus for electrochemical measurements, including AC impedance and current-voltage curve (I-V curve). The single solid oxide electrolysers were investigated for direct hydrogen electrolysis. The H_2 yield was analyzed by gas chromatography (GC-2014, SHIMADEU, Japan) under each new different applied voltage.

3 RESULTS AND DISCUSSION

3. 1 Analysis of the crystal structure

Fig. 1 shows the XRD patterns of the oxide powers at 1300 ºC in air for 20 h, which confirms that the perovskite-type $SrFeO_3$ and SFZO are pure phase. However, the phase transition from cubic perovskite to orthorhombic structure ($Sr_2Fe_2O_5$) has been observed for $SrFeO_3$ sample after reduction[12], as shown in Fig. 1 (a), suggesting a weak phase stability in reducing atmosphere. In contrast, as shown in Fig. 1(b), no phase transitions or impurites are observed for SFZO even treated at 800 ºC in 5%H_2/Ar for 3 h. The partial replacement of Fe with Zr has effectively improved the phase stability of SFZO even in strong reducing atmosphere. According to the Scherrer Equation $L = K\lambda/\beta\cos\theta$[13], the crystal cell parameter of the oxidized SFZO is determined to be 3.908 Å, which is slightly smaller than that of the reduced SFZO (3.921 Å). This is because the Fe^{4+} (0.585 Å) is partially reduced to Fe^{3+} (0.645 Å), which may give rise to expansion of the cell volume as the oxygen loss is present after high temperature reduction.

3. 2 Oxygen vacancy and transition metal

Fig. 2(a) shows the TGA tests for the reduced SFZO from 320 to 1000 ºC (5 ºC min^{-1}) in air. In the range of 320～476 ºC, the weight increase is attributed to the oxidation of Fe^{3+} to its higher valent state (Fe^{4+})[14] with consequent oxygen gain as the same time, accompanied by the 0.156 mol oxygen gain per chemical formula. In the range of 476～1000 ºC, an increased weight loss is observed, which is ascribed to the reduction of Fe^{4+} to Fe^{3+} as well as the loss of lattice oxygen, accompanied by the 0.121 mol oxygen loss per chemical formula at high temperature. The thermally induced lattice oxygen loss creates oxygen vacancies over 476 ºC. As a

result, to maintain the charge balance, the valence state of Fe ions changes from 4+ to 3+[15-17]. Fig. 2(b) shows the typical microstructures and lattice constant of the obtained SFZO powders. The lattice constant is 0.383 nm, presenting a similar lattice constant as reported for the (111) plane[18, 19].

In order to confirm the change in elemental valence, XPS analysis is performed to test the oxidized and reduced SFZO samples, respectively. All XPS patterns are fitted using a Shirley-type background subtraction method and the background functions for different spectra of different elements are fitted using 80% Gaussian and 20% Lorentzian functions[20]. All information of XPS peak comes from the database of Thermo Fisher Scientific[21]. As shown in Fig. 3(a), the Fe 2*p* spectrum can be deconvoluted with three spinorbital doublet pairs that are originated from different chemical coordination of Fe. The first one is at binding energies of 709.9 eV (Fe 2*p*3/2) and 722.78 eV (Fe 2*p*1/2), corresponding to Fe^{2+} ions; the second one is at 710.4 eV (Fe 2*p*3/2) and 723.5 eV (Fe 2*p*1/2), corresponding to the average valence state of Fe between 2+ and 3+; and the third one is at 711.4 eV (Fe 2*p*3/2) and 725.08 eV (Fe 2*p*1/2), assigned to Fe^{4+}. In Fig. 3(b), the Fe^{2+} (2*p*3/2), Fe^{3+} (2*p*3/2), Fe^{2+} (2*p*1/2) and Fe^{3+} (2*p*1/2) peaks are observed at 714.70, 711.88, 728.08 and 724.88 eV in the reduced SFZO sample, respectively. According to the fitting results, the ratio of Fe^{2+} and Fe^{3+} is about 2.1 in the reduced SFZO sample. Moreover, the shift of Fe binding energy between oxidized and reduced samples is attributed to the iron valence state change of Fe^{3+} to Fe^{4+}. In the meantime, the amount of oxygen lattice changes, which is consistent with the result of TGA analysis[22, 23].

3. 3 Electrical and electrochemical properties

The conductivity with a positive temperature coefficient for SFZO is shown in Fig. 4(a). The conductivities increase with the temperature and finally reach approximate 7.0 Scm^{-1} in air and 1.5 Scm^{-1} in 5%H_2/Ar, respectively. It should be noted that the conductivity of reduced SFZO is higher than the reported values for LSCM at high temperatures[24]. Fig. 4(b) shows the dependence of conductivity on oxygen partial pressure where the conductivity increases from 0.3 to 7.0 S cm^{-1}, with the oxygen partial pressure ranging from 10^{-17} to 10^{0} atm at 800 °C. A typical p-type conduction has been demonstrated for the SFZO oxide while small n-type conduction is still observed at low oxygen partial because of the reversible change between Fe^{4+}, Fe^{3+} and Fe^{2+}. The decrease of conductivity in the reducing atmosphere is ascribed to the decrease of concentration of charge carrier at low oxygen partial pressure atmosphere that leads to the generation of oxygen vacancy.

Fig. 5(a) and (b) show the AC impedance plots of symmetric cells with a configuration of SFZO-SDC/YSZ/SFZO-SDC tested under hydrogen and oxygen partial pressure, respectively. The ohmic

resistance (R_s) of impedance spectra is subtracted for the comparison of electrode polarization resistances. The intercept with real axis in the impedance spectra corresponds to the electrode polarization resistance (R_p), measured by Zview software[25]. As shown in Fig. 5(a), the R_p of the symmetric cell decreases from 5.74 to 2.29 Ω cm^2 with the hydrogen partial pressure ranging from 5 to 100%, suggesting that reducing atmosphere benefits the electrode polarization improving. In Fig. 5(b), the electrode polarization resistance is 0.71, 0.51, 0.39 and 0.3 Ω cm^2 under 2, 5, 10 and 20% O_2, respectively. This result indicates that SFZO can be a potentially promising candidate as cathode or anode in SOECs.

Fig. 6(a) shows the microstructure of a single electrolyser with the configuration of (cathode) SFZO-SDC/YSZ/LSM-SDC (anode). It can be found that the two porous electrode layers are approximately 10 μm in thickness, and adhere well to the YSZ electrolyte. The steam electrolysis was performed at different applied voltages with 5%H_2O/5%H_2/Ar and 5%H_2O/Ar fed into the cathode, ranging from 1.0 to 2.0 V at 800 °C, respectively. Fig. 6(b) shows the typical curves of the current density *versus* voltage (I-V curves) of the electrolysers for direct steam electrolysis. In order to check the sealing of single solid oxide electrolyser, the open circuit voltage (OCV) is recorded. The OCV of the solid oxide electrolyser reaches about 100 mV when cathode is fed with 5%H_2O/Ar while OCV reaches 1.1 V fed with 5%H_2O/5%H_2/Ar at 800 °C, which reflects a reasonable separation between anodic and cathodic gases. There exist two different cell processes in the voltage region: (a) the electrochemical reduction of cathodes and the oxidation of anodes at low voltages; (b) the steam electrolysis at high voltages. Above 1.1 V, the current densities increase steeply with both two different atmospheres fed in the SFZO cathode, which indicates that the SFZO electrode with zircoium doping significantly promotes the phase stability, resulting in good cell performances under reducing atmosphere. The current density of the solid oxide electrolyser based on the SFZO composite cathode fed with 5%H_2O/Ar increases from about 7.8 to 325 mA cm^{-2}, with the applied potential ranging from 1.0 to 2.0 V. The maximum current density reaches 326 mA cm^{-2} at 2.0 V when 5%H_2O/5%H_2/Ar is fed into cathode. All of the above indicates that the SFZO-SDC electrode shows a good cell performance for steam electrolysis even under reducing atmosphere.

To further study the electrochemical performance of electrodes, *in situ* AC impendence spectroscopy was used to investigate the polarization resistance of the cells under different applied voltages. Fig. 7 shows the *in situ* AC impedance spectroscopy of the electrolysis cells based on SFZO under different applied voltages ranging from 1.2 to 1.7 V at 800 °C in 5%H_2O/5%H_2/Ar and 5%H_2O/Ar, respectively. Two main

electrochemical processes (cathode reduction at low voltages and steam electrolysis at high voltages) exist in the range of 1.2~1.7 V during the electrolysis process under both two different atmospheres. As shown in Fig. 7 (a1, a2) in 5%H_2O/5%H_2/Ar, R_p values considerably decrease with the applied voltage increasing from 1.2 to 1.7 V. The increasing applied voltage can electrochemically reduce the cathode, which increases the mixed conductivity of SFZO, and accordingly enhances the electrode performance as well. Two semicircles are noted on the impedance spectroscopy: the high-frequency arcs (R_1) at high frequencies and low-frequency arcs (R_2) at low frequencies. The R_1 of the solid oxide electrolysers based on SFZO cathode is stable in 5%H_2O/5%H_2/Ar, indicating that the charge transfer at high frequency remains stable. At low frequency, the R_2 is slightly decreased from 3.74 to 3.67 Ω cm^2 at the applied voltage of 1.2~1.7 V, suggesting the improved kinetics of gas conversion. Fig. 7 (b1, b2) shows the *in situ* AC impendence spectroscopy of the SFZO-SDC composite cathode in 5%H_2O/Ar atmosphere. A similar phenomenon is observed in the less reducing atmosphere, which reveals that there are appropriate amounts of oxygen vacancies in the 5%H_2O/Ar atmosphere.

Fig. 8(a) and (b) show the electrolysis performances of SFZO cathodes fed with 5%H_2O/5%H_2/Ar and 5%H_2O/Ar at 800 °C, respectively. The current density with 5%H_2O/5%H_2/Ar fed into the cathode reaches approximate 78, 207 and 265 mA cm^{-2} at 1.2, 1.6 and 1.8 V, respectively. Similarly, the current density with 5%H_2O/Ar fed into cathode arrives to 98, 212 and 266 mA cm^{-2} at 1.2, 1.6 and 1.8 V, respectively. It is quite obvious that the SFZO cathode demonstrates similar performances in two different atmospheres. Moreover, the SFZO shows a stable performance in a wide range of applied voltage, indicating reasonable phase stability under a stronger reducing atmosphere at high temperature. The performance of SFZO is comparable to the reported values of 41~173 mA cm^{-2} at 1.2~2.0 V at 800 °C for a 2-mm-thick YSZ electrolyte supported electrolyser with 6 wt-% Co_3O_4-loaded LSM-BCZYZ cathode[26].

Fig. 8(c) and (d) show the rate of hydrogen production and the current efficiency of electrolysers based on SFZO composite cathode for steam electrolysis in 5%H_2O/5%H_2/Ar and 5%H_2O/Ar at different applied voltages at 800 °C, respectively. The hydrogen production rates reach as high as 0.7~1.4 mL cm^{-2} min^{-1} for the cell at 1.2~2.0 V in 5%H_2O/5%H_2/Ar atmosphere. In contrast, the hydrogen production rates get to 0.7~1.9 mL cm^{-2} min^{-1} in 5%H_2O/Ar under the same conditions, which are around 30% higher than the performance in former 5%H_2O/5%H_2/Ar atmosphere. Similarly, the current efficiency reaches 80% in 5%H_2O/Ar atmosphere while only 70% is achieved in 5%H_2O/5%H_2/Ar with the applied voltage ranging from 1.6 to 2.0 V. However,

the current efficiency reaches as high as 90% at low voltages with SFZO cathode in 5%H_2O/5%H_2/Ar because of the high catalytic activity in stronger reducing atmosphere. As we know, the SFZO is a typical p-type conductor and the conductivity in oxidizing atmosphere is around 1 order of magnitude higher than that in the reducing atmosphere. Similarly, the SFZO cathode is expected to demonstrate a lower conductivity in 5%H_2O/5%H_2/Ar than that in 5%H_2O/Ar atmosphere, which may be the reason why the cell with SFZO cathode in 5%H_2O/Ar shows higher current efficiency at high voltages.

4 CONCLUSION

In this work, perovskite SFZO oxide is reported as a redox-stable cathode for solid oxide steam electrolyser. Excellent phase stability is achieved even only 10% Zr is doped to the Fe-based perovskite oxide, with appropriate number of oxygen vacancies. Electrical property measurements show that the SFZO is a typical conductor with 1.5 and 7.0 S cm^{-1} in 5%H_2/Ar and air at 800 °C. SFZO oxide exhibits superior SOEC cathode performance, and the current efficiency as high as 90% is achieved for steam electrolysis in 5%H_2O/5%H_2/Ar at low voltages. All of above indicates the enormous potential of SFZO in direct steam electrolysis.

REFERENCES

(1) Patrakeev, M. V.; Mitberg, E. B.; Lakhtin, A. A.; Leonidov, I. A.; Kozhevnikov, V. L.; Kharton, V. V.; Avdeev, M.; Marques, F. M. B. Oxygen nonstoichiometry, conductivity, and seebeck coefficient of $La_{0.3}Sr_{0.7}Fe_{1-x}Ga_xO_{2.65+\delta}$ perovskites. *J. Solid State Chem.* **2002**, 157, 203–213.

(2) Alonso, J. A.; Mart ńez-Lope, M. J.; Casais, M. T.; MacManus-Driscoll, J. L.; Silva, P. S. I. P. N.; Cohen, L. F.; Fern ández-D áz, M. T. Non-stoichiometry, structural defects and properties of $LaMnO_{3+\delta}$ with high values ($0.11 \leqslant \delta \leqslant 0.29$). *J. Mater. Chem.* **1997**, 7, 2139–2144.

(3) Eichel, R. Structural and dynamic properties of oxygen vacancies in perovskite oxide-analysis of defect chemistry by modern multi-frequency and pulsed EPR techniques. *Phys. Chem. Chem. Phys*. **2011**, 13, 368–384.

(4) Jaiswal, S. K.; Kumar, J. Oxygen permeation characteristics of sol-gel derived barium-substituted strontium ferrite membranes. *J. Am. Ceram. Soc*. **2017**, 100, 1306–1312.

(5) Kanhere, P.; Chen, Z. A review on visible light active perovskite-based photocatalysts. *Molecules* **2014**, 19, 19995–20022.

(6) Ahmed, T.; Chen, A.; Yarotski, D. A.; Trugman, S. A.; Jia, Q.; Zhu, J. X. Magnetic, electronic, and optical properties of double perovskite Bi_2FeMnO_6. *Apl. Mater*. **2017**, 5, 35601–35608.

(7) Gan, L. Z.; Xie, K. Electricity storage with high roundtrip efficiency in a reversible solid oxide cell stack. *Chin. J. Chem. Phys*. **2016**, 29, 517–522.

(8) Ye, L. T.; Zhang, M. Y.; Huang, P.; Guo, G. C.; Hong, M. C.; Li, C. S.; Irvine, J. T. S.; Xie, K. Enhancing CO_2 electrolysis through synergistic control of non-stoichiometry and doping to tune cathode surface structures. *Nat. Commun*. **2017**, 8, 14785–14794.

(9) Patrakeev, M. V.; Leonidov, I. A.; Kozhevnikov, V. L.; Kharton, V. V. Ion-electron transport in strontium ferrites: relationships with structural features and stability. *Solid State Sci*. **2004**, 6, 907–913.

(10) Li, Z.; Li, S. S.; Tseng, C. J.; Tao, S. W.; Xie, K. Redox-reversible perovskite ferrite cathode for high temperature solid oxide steam electrolyser. *Electrochim. Acta* **2017**, 229, 48–54.

(11) Kostogloudis, G. C.; Ftikos, C. Properties of A-site-deficient $La_{0.6}Sr_{0.4}Co_{0.2}Fe_{0.8}O_{3-\delta}$-based perovskite oxides. *Solid State Ionics* **1999**, 126, 142–151.

(12) Santos-Gómez, L.; Compana, J. M.; Bruque, S.; Losilla, E. R.; Marrero-López, D. Symmetric electrodes for solid oxide fuel cells based on Zr-doped $SrFeO_{3-\delta}$. *J. Power Sources* **2015**, 279, 419–427.

(13) Monshi, A.; Foroughi, M. R.; Monshi, M. R. Modified Scherrer equation to estimate more accurately nano-crystallite size using XRD. *World J. Nano. Sci. Eng*. **2012**, 2, 154–160.

(14) David, N. M.; Roger, A. D. S.; Han-Ill, Y.; Manfred, M. Phase stability and oxygen nonstoichiometry of highly oxygen-deficient perovskite-type oxides: a case study of (Ba, Sr)(Co, Fe)$O_{3-\delta}$. *Chem. Mater*. **2012**, 24, 269–274.

(15) Patra, H.; Rout, S. K.; Pratihar, S. K.; Bhattacharya, S. Thermal, electrical and electrochemical charateristics of $Ba_{1-x}Sr_xCo_{0.8}Fe_{0.2}O_{3-\delta}$ cathode material for intermediate temperature solid oxide fuel cells. *Int. J. Hydrogen Energy* **2011**, 36, 11904–11923.

(16) Li, Z.; Wei, B.; Lu, Z.; Huang, X.; Su, W. Structure, electrical and thermal properties of $(Ba_{0.5}Sr_{0.5})_{1-x}Gd_xCo_{0.8}Fe_{0.2}O_{3-\delta}$ perovskite as a solid-oxide fuel cell cathode. *Solid State Ionics* **2012**, 207, 38–43.

(17) Zhang, Z.; Chen, D.; Shao, Z. Efficient and CO_2-tolerant oxygen transport membranes prepared from high-valence B-site substituted cobalt-free $SrFeO_{3-\delta}$. *J. Memb. Sci*. **2015**, 495, 187–197.

(18) Ghaffari, M.; Huang, H.; Tan, O. K.; Shannon, M. Band gap measurement of by ultraviolet photoelectron spectroscopy and photovoltage method. *Cryst. Eng. Comm*. **2012**, 14, 7487–7492.

(19) Xiao, G.; Liu, Q.; Wang, S.; Komvokis, V. G.; Amiridis, M. D.; Heyden, A.; Ma, S.; Chen, F. Synthesis and characterization of Mo-doped $SrFeO_{3-\delta}$ as cathode materials for solid oxide fuel cells. *J. Power Sources* **2012**, 202, 63–69.

(20) Qin, Q.; Wu, G.; Chen, S.; Doherty, W.; Xie, K.; Wu, Y. Perovskite titanate cathode decorated by in-situ grown iron nanocatalyst with enhanced electrocatalytic activity for high-temperature steam electrolysis. *Electrochim. Acta* **2014**, 127, 215–227.

(21) Zhang, J.; Xie, K.; Zhang, Y.; Yang, L.; Wu, G.; Qin, Q.; Li, Y.; Wu, Y. Composite titanate cathode decorated with heterogeneous electrocatalytic sites towards efficient carbon dioxide electrolysis. *RSC Adv*. **2014**, 4, 22697–22709.

(22) Yuan, H.; Zhang, L.; Xu, M.; Du, X. Effect of sol pH on microstructures, optical and magnetic properties of (Co, Fe)-codoped ZnO films synthesized by sol-gel method. *J. Alloy Compd*. **2015**, 651, 571–577.

(23) Lashtabeg, A.; Irvine, J. T. S.; Feighery, A. Thermomechanical and conductivity studies of doped niobium titanates as possible current collector material in the SOFC anode. *Ionics* **2003**, 9, 220–226.

(24) Ruan, C.; Xie, K. A redox-stable chromate cathode decorated with in situ grown nickel nanocatalyst for efficient carbon dioxide electrolysis. *Catal. Sci. Technol*. **2015**, 5, 1929–1940.

(25) Xu, S.; Dong, D.; Wang, Y.; Doherty, W.; Xie, K. Perovskite chromates cathode with resolved and anchored nickel nano-particles for direct high-temperature steam electrolysis. *J. Power Sources* **2014**, 246, 346–355.

(26) Li, S.; Yan, R.; Wu, G.; Xie, K.; Cheng, J. Composite oxygen electrode LSM-BCZYZ impregnated with Co_3O_4 nanoparticles for steam electrolysis in a proton-conducting solid oxide electrolyzer. *Int. J. Hydrogen Energy* **2013**, 38, 14943–14951.

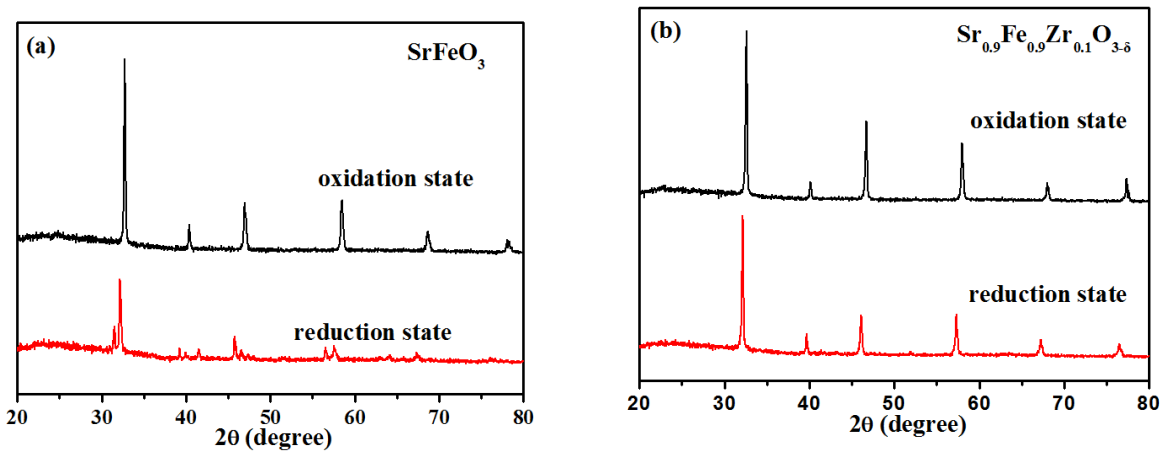

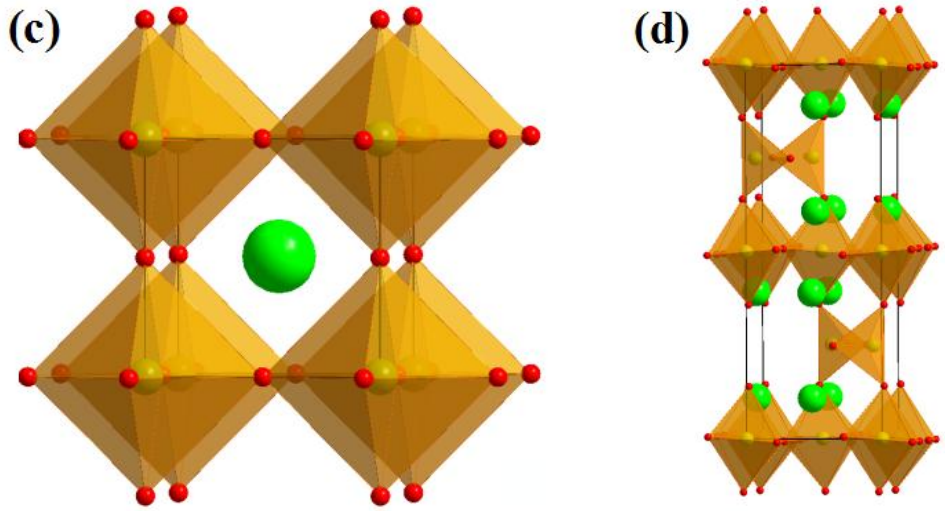

Fig. 1. XRD patterns of the samples (a) oxidized and reduced $SrFeO_3$; (b) oxidized and reduced SFZO. The diagram of (c) cubic perovskite and (d) orthorhombic structure (where A is Sr, green; B is Fe/Zr, yellow; and O is oxygen, red)

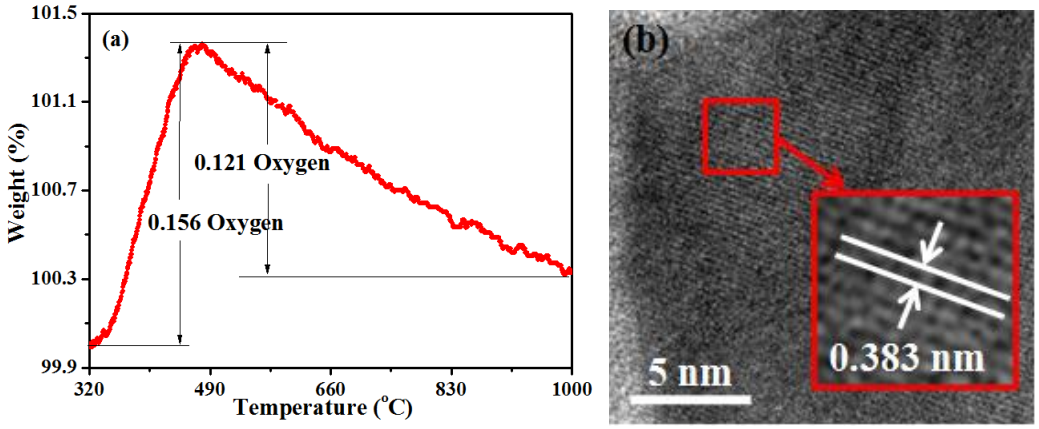

Fig. 2. (a) TGA tests of reduced SFZO from 320 to 1000 ºC in air; (b) TEM image of the reduced SFZO sample

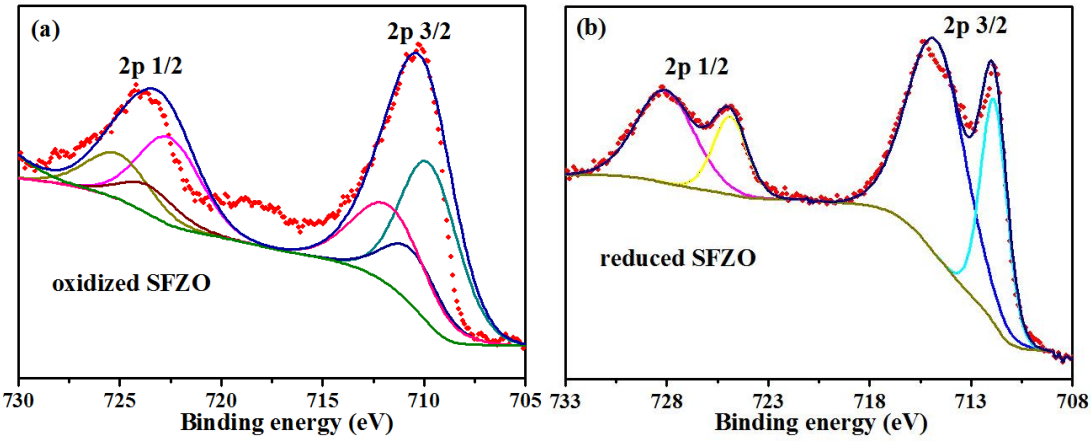

Fig. 3. XPS results of Fe in (a) oxidized SFZO and (b) reduced SFZO sample

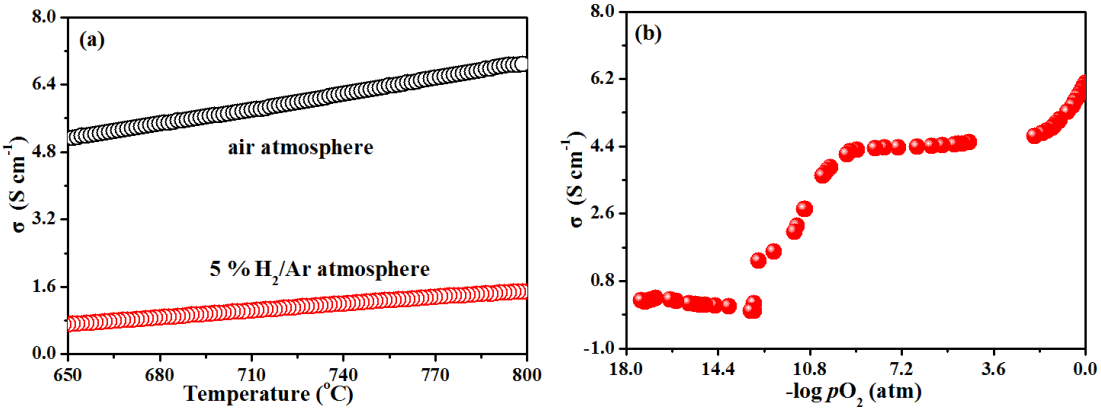

Fig. 4. Dependences of the conductivity of SFZO on (a) the temperature in air and in 5%H₂/Ar from 650 to 800 °C; (b) Oxygen partial pressure ranging from 10^{0} to 10^{-17} atm at 800 °C, respectively

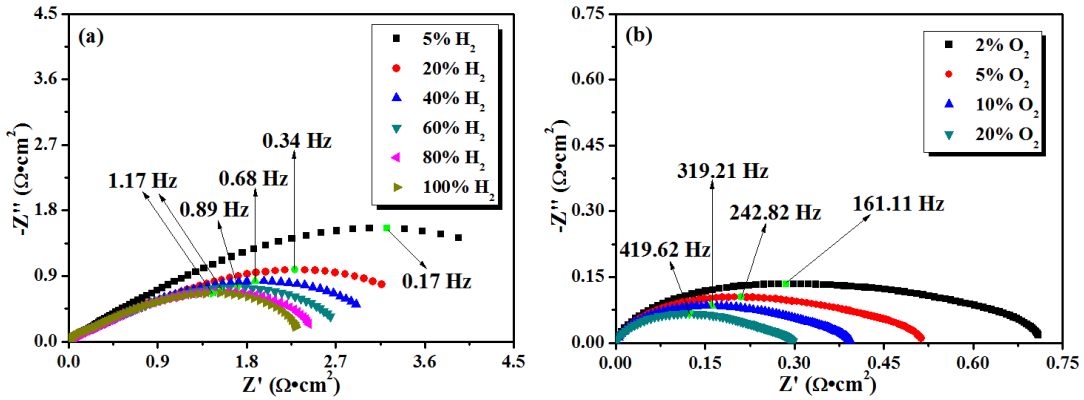

Fig. 5. AC impedance of symmetric cells based on SFZO electrodes tested at 800 °C under (a) different hydrogen partial pressures and (b) different oxygen partial pressures, respectively

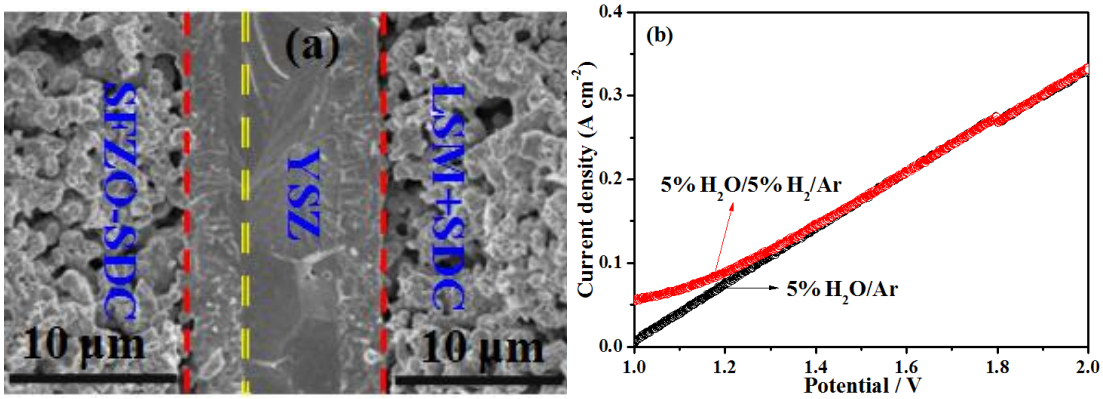

Fig. 6. (a) SEM image of the electrolyzer cells: SFZO-SDC/YSZ/LSM-SDC; (b) the I-V curves of the solid oxide electrolyzer based on SFZO composite oxygen electrode for steam electrolysis at 800 °C in two different atmosphere 5%H₂O/5%H₂/Ar and 5%H₂O/Ar

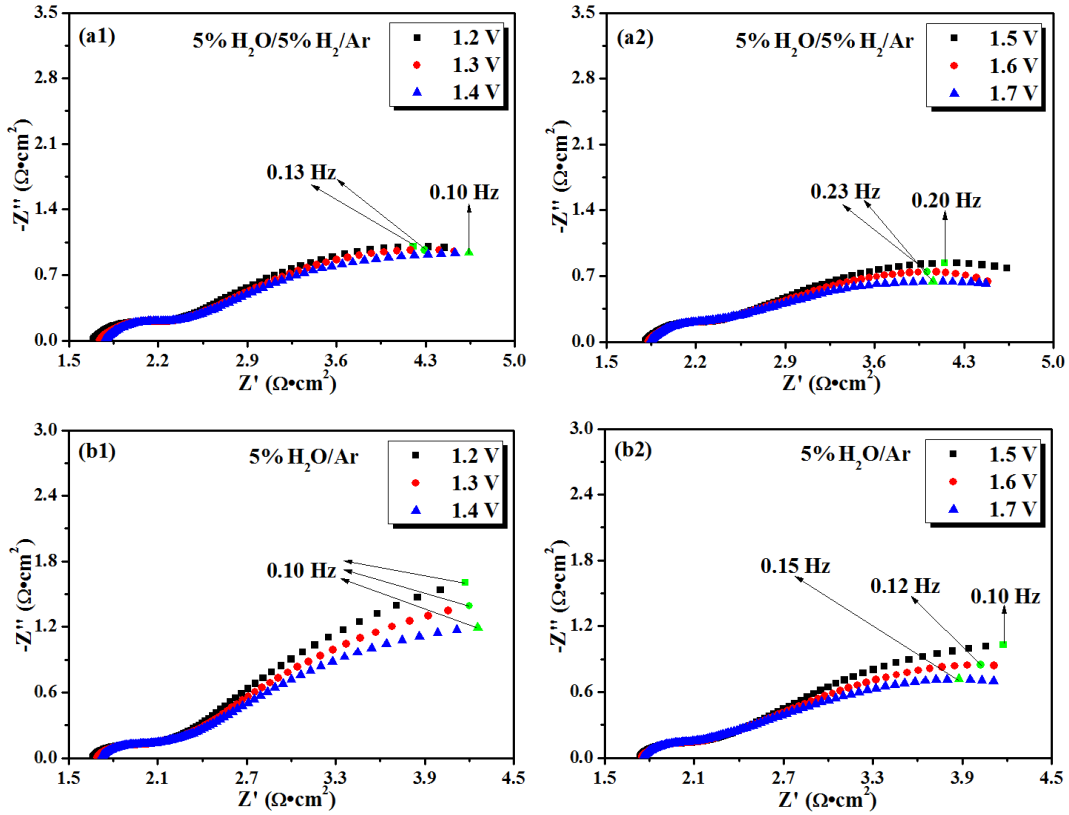

Fig. 7. ***In situ*** **AC impendence of the solid oxide symmetric electrolyzers based on SFZO at 800 ºC with the flow of 5%H_2O/5%H_2/Ar (a1, a2) and 5%H_2O/Ar (b1, b2)**

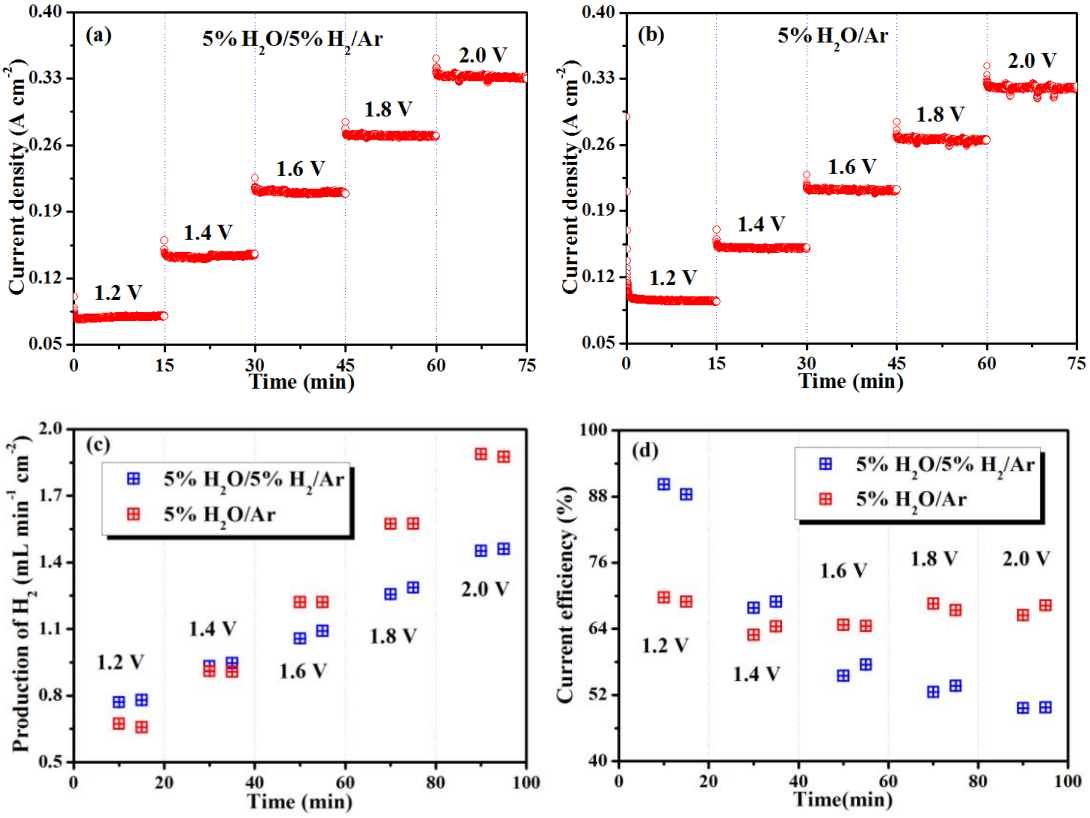

Fig. 8. Performances of single electrolyzer with cathode based on SFZO at different applied potentials for steam electrolysis in different atmospheres: (a) 5%H_2O/5%H_2/Ar and (b) 5%H_2O/Ar. The hydrogen production

(c) and current efficiency (d) for the electrolyzers with the flow of 5%H_2O/5%H_2/Ar and 5%H_2O/Ar at 800 ºC

Perovskite $Sr_{0.9}Fe_{0.9}Zr_{0.1}O_{3-\delta}$: Redox-stable Structure, Oxygen Vacancy, Electrical Properties and Steam Electrolysis Performance

LI Zhe(李　哲)　YE Ling-Ting(叶灵婷)　XIE Kui(谢　奎)

In this study, $Sr_{0.9}Fe_{0.9}Zr_{0.1}O_{3-\delta}$ (SFZO) is synthesized and then treated in 5%H_2/Ar and air at high temperature, exhibiting excellent redox stability. Redox-stable structure, oxygen vacancy and electrical properties of the SFZO are investigated. Steam electrolysis is then performed with SFZO cathode under 5%H_2O/5%H_2/Ar and 5%H_2O/Ar atmospheres, respectively. The present results indicate that the SFZO is a novel promising cathode material for solid oxide steam electrolyser.